P H Y S I C A L   R E V I E W   L E T T E R S

Temporal Dynamics of Photon Pairs Generated by an Atomic Ensemble

S. V. Polyakov, C. W. Chou, D. Felinto, and H. J. Kimble

Norman Bridge Laboratory of Physics 12-33, California Institute of Technology, Pasadena, California 91125, USA

The time dependence of nonclassical correlations is investigated for two fields $(1, 2)$ generated by an ensemble of cold cesium atoms via the protocol of Duan *et al.* [Nature (London) **414**, 413 (2001)]. The correlation function $R(t_1, t_2)$ for the ratio of cross to autocorrelations for the $(1, 2)$ fields at times (t_1, t_2) is found to have a maximum value $R^{max} = 292 \pm 57$, which significantly violates the Cauchy-Schwarz inequality $R \leq 1$ for classical fields. Decoherence of quantum correlations is observed over $\tau_d \simeq 175$ ns, and is described by our model, as is a new scheme to mitigate this effect.

In recent years quantum measurement combined with conditional quantum evolution has emerged as a powerful paradigm for accomplishing diverse tasks in quantum information science [1–4]. For example, Duan, Lukin, Cirac, and Zoller (DLCZ) [4] have proposed a scheme for scalable quantum communication networks that relies upon a probabilistic entanglement between remotely located atomic ensembles. By utilizing successful measurements to condition subsequent steps in the protocol, DLCZ have developed a scheme that has built-in quantum memory, entanglement purification, and resilience to realistic noise sources, enabling a quantum repeater architecture to overcome photon attenuation [5,6].

Central to the DLCZ protocol is the ability to *write* and *read* collective spin excitations *into* and *out of* an atomic ensemble, with efficient conversion of discrete spin excitations to single-photon wave packets. Observations of the resulting nonclassical correlations between the optical fields generated from *writing* and *reading* such spin excitations have recently been reported both at the single-photon level [7–11] as appropriate to the protocol of DLCZ and in a regime of large photon number $n \sim 10^3$–10^7 [12]. Generation and detection efficiencies have now been improved so that excitation stored within an atomic ensemble can be employed as a controllable source for single photons [8].

A critical aspect of such single-photon wave packets is that they are emitted into well defined spatiotemporal modes to enable quantum interference between emissions from separate ensembles (e.g., for entanglement based quantum cryptography [4]). However, with the exception of the verification of the time delay implicit for the Raman processes employed [12], experiments to date have not investigated the detailed time and spatial dependence of quantum correlations for the emitted fields from the atomic ensemble. The high efficiencies achieved in Ref. [8] now enable such an investigation for the temporal properties of nonclassical correlations between emitted photon pairs, which we report in this Letter.

We study the time dependence of quantum correlations for photons emitted from an ensemble of cold cesium

atoms, with photon pairs created by classically controlled *write* and *read* pulses. We also map the decay of quantum correlations by varying the delay between the *write* and *read* pulses. We have developed a model to describe the decoherence and find good correspondence with our measurements. This model is utilized to analyze a new proposal that should extend the correlation times to beyond 10 μs, which would allow for entanglement between atomic ensembles on the scale of several kilometers.

The DLCZ scheme is implemented in an optically thick sample of four-level atoms, cooled and trapped in a magneto-optical trap (MOT). In particular, we utilize the ground hyperfine levels $6S_{1/2}, F = \{4; 3\}$ of Cs (labeled $\{|a\rangle; |b\rangle\}$), and excited levels $\{6P_{3/2}, F = 4; 6P_{1/2}, F = 4\}$ of the D_2, D_1 lines (labeled $\{|e\rangle; |e'\rangle\}$). Our experimental procedure is illustrated in Fig. 1. An initial *write* pulse at 852 nm creates a state of collective excitation in an atomic
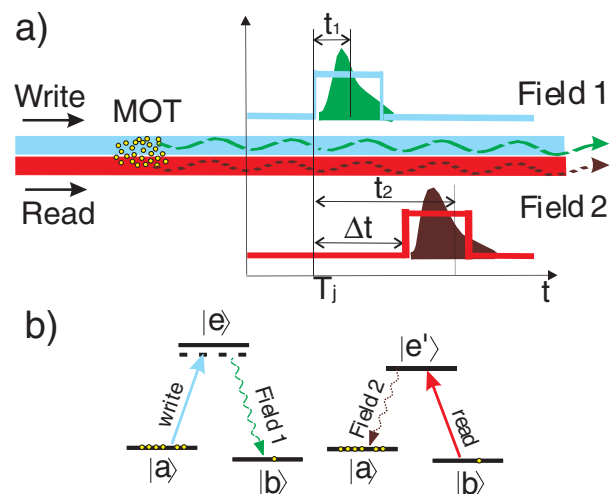

FIG. 1 (color online).   (a) Schematic of experiment. *Write* and *read* pulses propagate into a cloud of cold Cs atoms (MOT) at times T_j and $T_j + \Delta t$, respectively, and generate the correlated output fields 1 and 2. Quantum correlations for these fields at times (t_1, t_2) are investigated by way of photoelectric detection. (b) The relevant atomic level scheme.

263601-1

ensemble, as heralded by a photoelectric detection from
the Raman field 1. After a user-programmable delay Δt, a
read pulse at 894 nm converts this atomic excitation into a
field excitation of the Raman field 2. The (*write, read*)
pulses are approximate coherent states with mean photon
numbers (10^3, 10^5), respectively, focused into MOT as
Gaussian beams with orthogonal polarizations and beam
waist $w_0 = 30$ μm.

Each attempt to generate a correlated pair of photons in
the (1, 2) fields is preceded by shutting off the trapping
light for 700 ns. The repumping light is left on for an
additional 300 ns in order to empty the $|b\rangle$ state, thus
preparing the atoms in $|a\rangle$. The *j*th trial of a protocol is
initiated at time T_j when a rectangular pulse from the *write*
laser beam, 150 ns in duration and tuned 10 MHz below the
$|a\rangle \rightarrow |e\rangle$ transition, induces spontaneous Raman scatter-
ing to level $|b\rangle$ via $|a\rangle \rightarrow |e\rangle \rightarrow |b\rangle$. The *write* pulse is
weak so that the probability to scatter one Raman photon
into a forward propagating wave packet is much less than
unity for each pulse. Detection of one photon from field 1
results in a "spin" excitation to level $|b\rangle$, with this excita-
tion distributed in a symmetrized, coherent manner
throughout the sample of N atoms illuminated by the *write*
beam [4]. Regardless of detection of a photon in field 1, we
next address the ensemble with a *read* pulse at a time $T_j +$
Δt, where Δt is controlled by the user. The *read* light is a
rectangular pulse, 120 ns in duration, resonant with the
$|b\rangle \rightarrow |e'\rangle$ transition.

To address the photon statistics, we use four avalanche
photodetectors, a pair for each field (1, 2), activated at
$(T_j, T_j + \Delta t)$, respectively, for 200 ns for all experiments.
We define $p_\tau(t_l, t_m)$ as the joint probability for photoelec-
tric detection from field l in the interval $[T_j + t_l, T_j + t_l +$
$\tau]$ and for detection from field m in the interval $[T_j +$
$t_m, T_j + t_m + \tau]$ in a temporal bin τ; l and m equal 1 or 2.
$p_\tau(t_l, t_m)$ is determined from the record of time-stamped
detection events of all four photodetectors, allowing us to
measure autocorrelations and cross correlations simulta-
neously. Similarly, $q_\tau(t_l, t_m)$ gives the joint probability for
detection for fields (l, m) in the intervals $([T_j + t_l, T_j +$
$t_l + \tau], [T_k + t_m, T_k + t_m + \tau])$ for two trials $k \neq j$.

Following Refs. [7,8], we introduce the time-dependent
ratio $R_\tau(t_1, t_2)$ of cross correlation to autocorrelation for
the (1, 2) fields, where

$$R_\tau(t_1, t_2) \equiv \frac{[p_\tau(t_1, t_2)]^2}{p_\tau(t_1, t_1)p_\tau(t_2, t_2)}. \quad (1)$$

This ratio is constrained by the inequality $R_\tau(t_1, t_2) \leq 1$ for
all fields for which the Glauber-Sudarshan phase-space
function is well behaved (i.e., *classical* fields) [7,13].
Beyond enabling a characterization of the quantum char-
acter of the (1, 2) fields in a model independent fashion,
measurements of $R_\tau(t_1, t_2)$ also allow inferences of the
quantum state for collective excitations of single spins
within the atomic ensemble.

The first step in the determination of $R_\tau(t_1, t_2)$ is the
measurement of the joint probability $p_\tau(t_1, t_2)$ for the (1, 2)
fields, and, for comparison, $q_\tau(t_1, t_2)$ for independent trials.
In our experiment, we focus on two cases: (I) nearly si-
multaneous application of *write* and *read* pulses with offset
$\Delta t = 50$ ns less than the duration of either pulse, and (II)
consecutive application of *write* and *read* pulses with $\Delta t =$
200 ns longer than the *write, read* durations. Results for
$p_\tau(t_1, t_2)$ and $q_\tau(t_1, t_2)$ are presented in Fig. 2 as functions
of the detection times (t_1, t_2) for the fields (1, 2). For both
$\Delta t = 50$ and 200 ns, $p_\tau(t_1, t_2) \gg q_\tau(t_1, t_2)$, indicating the
strong correlation between fields 1 and 2, with the maximal
ratio $g_{1,2}^\tau(t_1, t_2) = p_\tau(t_1, t_2)/q_\tau(t_1, t_2) \gtrsim 30$, much greater
than reported previously [7–9]. In Fig. 2, $\tau = 4$ ns, leading
to statistical errors of $\approx 8\%$ for the largest values shown.

In case (I) for nearly simultaneous *write* and *read* pulses,
Fig. 2(a) shows that $p_\tau(t_1, t_2)$ peaks along the line $t_2 -$
$t_1 = \delta t_{12} \simeq 50$ ns with a width $\Delta t_2 \simeq 60$ ns, in correspon-
dence to the delay δt_{12} and duration Δt_2 for readout
associated with the transition $|b\rangle \rightarrow |e'\rangle \rightarrow |a\rangle$ given an
initial transition $|a\rangle \rightarrow |e\rangle \rightarrow |b\rangle$ [12]. Apparently, the
qualitative features of $p_\tau(t_1, t_2)$ depend only upon the
time difference between photon detections in fields (1, 2)
[i.e., $p_\tau(t_1, t_2) \approx F(t_2 - t_1)$]. In case (II) with the *read*
pulse launched 200 ns after the *write* pulse, excitation is
"stored" in the atomic ensemble until the readout. The
production of correlated photon pairs should now be dis-
tributed along $t_2 \simeq \Delta t + \delta t_{12}$ with width $\simeq \Delta t_2$. Instead, as
shown in Fig. 2(c), $p_\tau(t_1, t_2)$ peaks towards the end of the
write pulse (i.e., $t_1 \gtrsim 100$ ns), and near the beginning of
the *read* pulse (i.e., $200 \lesssim t_2 \lesssim 300$ ns). Early events for
field 1 lead to fewer correlated events for field 2, as
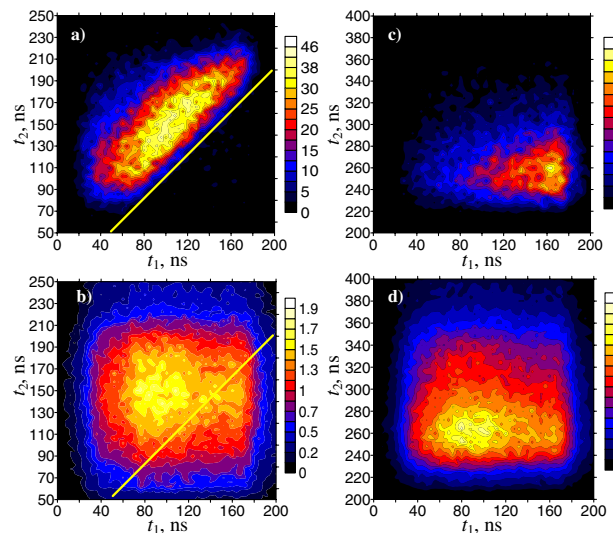

FIG. 2 (color online). Probability of joint detection scaled by
10^9 from fields (1, 2) at times (t_1, t_2) with $t_1 = t_2 = 0$ at the
beginning of the *write* pulse. (a) $p_\tau(t_1, t_2)$ and (b) $q_\tau(t_1, t_2)$ for
overlapped *write* and *read* pulses, $\Delta t = 50$ ns. The solid line
corresponds to $t_2 = t_1$. (c) $p_\tau(t_1, t_2)$ and (d) $q_\tau(t_1, t_2)$ for con-
secutive *write* and *read* pulses, $\Delta t = 200$ ns.

$p_\tau(t_1, t_2)$ decays rapidly beyond $t_2 - t_1 = \tau_d \simeq 175$ ns. The marked contrast between $p_\tau(t_1, t_2)$ for $\Delta t = 50$ and 200 ns results in a diminished ability for the conditional generation of single photons from excitation stored within the atomic ensemble [8] and for the implementation of the DLCZ protocol for increasing Δt. The underlying mechanism is Zeeman decoherence, as discussed below.

Figures 2(b) and 2(d) displays $q_\tau(t_1, t_2)$ for independent trials $j \neq k$. $q_\tau(t_1, t_2)$ is expected to be proportional to the product of intensities of the fields 1 and 2, in reasonable correspondence to the form shown in Figs. 2(b) and 2(d) for our roughly rectangular *write, read* pulses, but distinctively different from $p_\tau(t_1, t_2)$ in Figs. 2(a) and 2(c).

To deduce $R_\tau(t_1, t_2)$ from Eq. (1), we determine the joint detection probabilities $p_\tau(t_i, t_i)$ for fields 1 and 2 from the same record of photoelectric events. Since the rate of coincidences for autocorrelations is roughly 10^2 times smaller than for cross correlations for the $(1, 2)$ fields, we increase the bin size τ to 30 ns to accumulate enough events to reduce the statistical errors to acceptable levels. Figure 3 shows the time dependencies of $p_\tau(t_1, t_1)$ and $p_\tau(t_2, t_2)$ for cases (I) and (II). While the shape of $p_\tau(t_1, t_1)$ associated with the *write* pulse does not change with Δt, the profile of $p_\tau(t_2, t_2)$ from the *read* pulse is affected and exhibits a rise time that is ~ 3 times shorter for $\Delta t = 200$ ns than for $\Delta t = 50$ ns. This prompt rise in 3(b) is consistent with the observation that stored excitation is efficiently addressed at the beginning of the *read* pulse for nonoverlapping *write, read* pulses, while the longer rise time in 3(a) results from overlapping excitation and retrieval of atoms from the state $|b\rangle$.

We employ the data in Figs. 2 and 3 together with Eq. (1) to construct $R_\tau(t_1, t_2)$, presented in Fig. 4 [14]. Not unexpectedly, the trends for $R_\tau(t_1, t_2)$ closely resemble those of $p_\tau(t_1, t_2)$. We observe maximal violations of Cauchy-Schwarz inequality with $R_\tau^{\max} = 292 \pm 57$ for $\Delta t = 50$ ns and $R_\tau^{\max} = 202 \pm 60$ for $\Delta t = 200$ ns ($R_\tau = 198 \pm 33$ in the neighboring bin), where $R_\tau(t_1, t_2) \leq 1$ for classical fields [7,13]. The relatively large errors in $R_\tau(t_1, t_2)$ arise predominantly from the uncertainties in $p_\tau(t_1, t_1)$ and $p_\tau(t_2, t_2)$ (Fig. 3) [15].

The forms for $p_\tau(t_1, t_2)$ and $R_\tau(t_1, t_2)$ for the cases $\Delta t = 50$ and 200 ns imply a decoherence process operative on a time scale $\tau_d \sim 175$ ns. To investigate this decay, we performed a separate experiment with the delay Δt varied $0 \leq \Delta t \leq 400$ ns. For each Δt we determine the normalized correlation function $g_{1,2}^\tau$ from the ratio of integrated coincidence counts to singles counts over the entire detection window (i.e., $\tau = 200$ ns); see Fig. 5.

In Fig. 5, the initial growth of $g_{1,2}^\tau$ for small Δt is due to the finite time required to produce sequentially photons in the $(1, 2)$ fields, which is already evident in Fig. 2 and characterized by $\Delta t_2 \simeq 60$ ns. More troublesome is the rapid decay of $g_{1,2}^\tau$ over times $100-200$ ns. The form for

FIG. 4 (color online). The experimentally derived ratio $R_\tau(t_1, t_2)$ for the $(1, 2)$ fields, with $R_\tau \leq 1$ for classical fields. The left column gives (a) $R_\tau(t_1, t_2)$ for $\Delta t = 50$ ns and (b) $\Delta t = 200$ ns; the right column gives the associated statistical uncertainties. Bin size $\tau = 30$ ns.
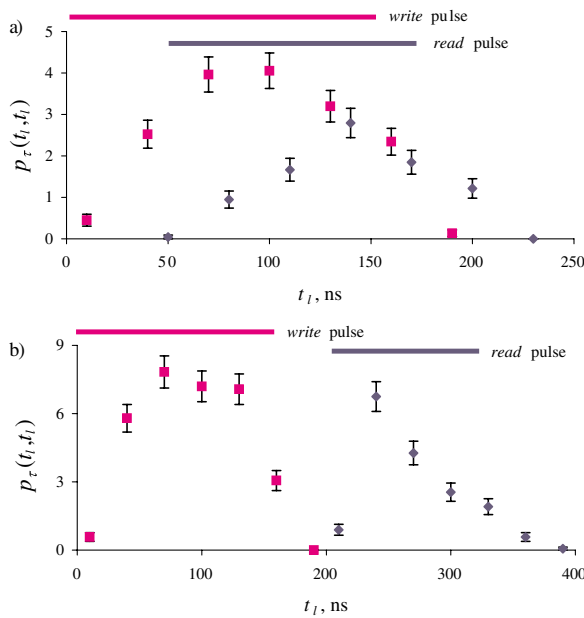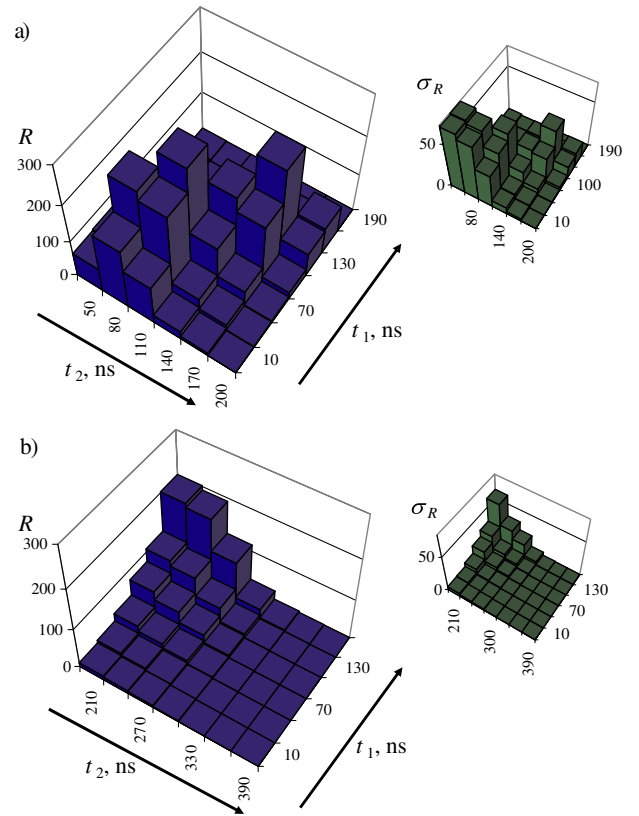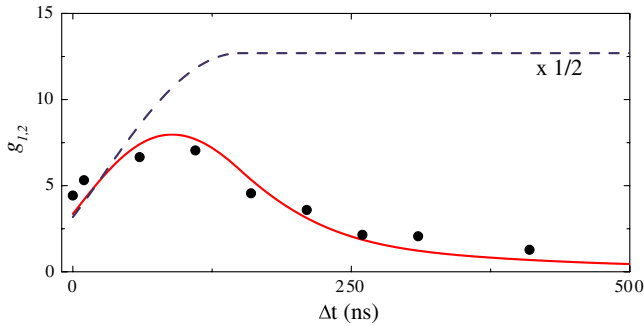

FIG. 3 (color online). Probability of joint detection scaled by 10^8, $p_\tau(t_1, t_1)$ for field 1 (squares) and $p_\tau(t_2, t_2)$ for field 2 (diamonds) as functions of respective detection times t_1 and t_2. Bin size $\tau = 30$ ns. (a) $\Delta t = 50$ ns; (b) $\Delta t = 200$ ns.

FIG. 5 (color online). Coherence time assessment. Experimentally acquired $g_{1,2}^\tau$ (black dots), comparison with the scaled $\tilde{p}_{1,2}(\Delta t)$ from theory (solid line), and prediction for a spin polarized $m_F = 0$ MOT (dotted line).

$g_{1,2}^\tau$ versus Δt in Fig. 5 motivates our choices $\Delta t = 50$ and 200 ns in Figs. 2–4. Note that $\Delta t \ll \Delta t_{12}$ would result in a substantial reduction in our $g_{1,2}^\tau$.

A likely cause of the quantum correlation decay is Larmor precession among the Zeeman states of the $F = 3, 4$ hyperfine levels of the $6S_{1/2}$ ground level. To investigate this possibility, we have extended the treatment of Ref. [16] to include the *readout* process as well as the full set of Zeeman states for $F = 3, 4$. The atomic ensemble is assumed to be initially unpolarized and uniformly distributed over MOT magnetic fields. With *write* and *read* pulses that approximate those used in our experiment and separated by Δt, we calculate the joint probability $p_{1,2}^{\text{th}}(\Delta t)$ to generate a pair of photons in the fields $(1, 2)$. We compare the quantity $\tilde{p}_{1,2}(\Delta t) \equiv \xi p_{1,2}^{\text{th}}(\Delta t)$ to the measured $g_{1,2}^\tau(\Delta t)$ by way of a single overall scaling parameter ξ for all Δt, as the rate of single counts in fields $(1, 2)$ is measured not to depend on Δt (to within 20%). The result is the solid curve in Fig. 5 that adequately describes the impact of Larmor precession on our experiment. The form of $\tilde{p}_{1,2}(\Delta t)$ strongly depends upon the inhomogeneity of Zeeman splitting across the MOT, which is described by the parameter $K = \mu_B g_{F_g} Lb/h$, where L is the MOT diameter, b is the gradient of the magnetic field for the MOT, and g_{F_g} is the Landé factor. The curve in Fig. 5 is the theoretical result for an initially unpolarized sample with $K = 1.1$ MHz as for our experiment (i.e., $L \approx 3.6$ mm and $b \approx 8.4$ G/cm).

A remedy for this dephasing is to switch off the MOT field, and transfer the sample to a dipole-force trap. Alternatively, we are developing a scheme that should allow for long coherence times even in the presence of the quadrupole field of the MOT by utilizing only magnetic-field insensitive states. The *write*, *read* beams are circularly polarized ($\sigma_\pm$) and are aligned along the z axis of the MOT, which provides the quantization axis. Atoms within the approximately cylindrical volume illuminated by these beams are initially spin polarized into $F = 4, m_F = 0$ [17], where m_F marks Zeeman sublevels. The $(1, 2)$ fields are selected to be $\sigma_\pm$, which results in spin

excitation stored in $F = 3, m_F = 0$. The prediction of our model for this new protocol for the same experimental conditions but with an initially spin polarized sample is the dashed curve in Fig. 5, resulting in an increase of more than $3\times$ in $g_{1,2}^\tau$, and significantly extending the decoherence time to more than $\tau_d \sim 10$ μs.

In conclusion, we have reported the first observations of the temporal dependence of the joint probability $p_\tau(t_1, t_2)$ for the generation of correlated photon pairs from an atomic ensemble, which is critical for the protocol of Ref. [4]. Our measurements of $p_\tau(t_1, t_2)$ are an initial attempt to determine the structure of the underlying two-photon wave packet [18]. The time dependence of the ratio $R_\tau(t_1, t_2)$ evidences the nonclassical character of the $(1, 2)$ fields with $R^{\max} = 292 \pm 57 \not\gtrless 1$. By contrast, previous measurements have reported $R \not\gtrless 1$ only for detection events integrated over the entire durations of the *write* and *read* pulses ($R = 1.84 \pm 0.06$ [7], $R = 1.34 \pm 0.05$ [9], and $R = 53 \pm 2$ [8]). Decoherence via Larmor precession is characterized and identified as a principal limitation of the current experiment. A new scheme for effectively eliminating this decay process is proposed and analyzed, and could be important for the experimental realization of scalable quantum networks [4] as well as for an improved source for single photons [8].

[1] C. H. Bennett *et al.*, Phys. Rev. Lett. **70**, 1895 (1993).
[2] R. Raussendorf and H. J. Briegel, Phys. Rev. Lett. **86**, 5188 (2001).
[3] E. Knill, R. Laflamme, and G. J. Milburn, Nature (London) **409**, 46 (2001).
[4] L.-M. Duan *et al.*, Nature (London) **414**, 413 (2001).
[5] H.-J. Briegel *et al.*, Phys. Rev. Lett. **81**, 5932 (1998).
[6] S. J. Enk, J. I. Cirac, and P. Zoller, Science **279**, 205 (1998).
[7] A. Kuzmich *et al.*, Nature (London) **423**, 731 (2003).
[8] C. W. Chou *et al.*, Phys. Rev. Lett. **92**, 213601 (2004).
[9] Wei Jiang *et al.*, Phys. Rev. A **69**, 043819 (2004).
[10] M. D. Eisaman *et al.*, quant-ph/0406093.
[11] D. N. Matsukevich and A. Kuzmich, Science **306**, 663 (2004).
[12] C. H. van der Wal *et al.*, Science **301**, 196 (2003).
[13] J. F. Clauser, Phys. Rev. D **9**, 853 (1974).
[14] Before applying Eq. (1), we reprocess the data for $p_\tau(t_1, t_2)$ in Fig. 2 for $\tau = 30$ ns bin size.
[15] To test the validity of our experiment, we verify $R(t_1^j, t_2^k) = 1$ to within statistical uncertainty $\leq 4\%$ for the $(1, 2)$ fields from different trials $j \neq k$.
[16] L.-M. Duan, J. I. Cirac, and P. Zoller, Phys. Rev. A **66**, 023818 (2002).
[17] Note that the beam waist for the *write, read* fields $w_0 = 30$ μm $\ll L$, where $L \approx 3.6$ mm gives MOT diameter.
[18] K. M. Gheri *et al.*, Fortschr. Phys. **46**, 401 (1998).